

Weighted density functional theory of the solvophobic effect

Sean X. Sun

Department of Chemistry, University of California, Berkeley, California 94720

(Received 24 July 2000; revised manuscript received 5 April 2001; published 24 July 2001)

We are interested in the spatial density of a molecular fluid in the presence of a solute of arbitrary size and shape. The density functional is written as the sum of a $F_0[\rho(\mathbf{r})]$ that effectively describes small deviations around the uniform density, plus an energy density part that is responsible for formation of liquid-vapor interface. Using the weighted density approach, we require the density functional to match with several observed properties of the fluid such as equation of state and surface tension. We also show that weighting functions for calculating the weighted density can be obtained from experimental data. Using these elements, we construct a spatial density functional theory of water and apply it to obtain densities and solvation energies of a hard-sphere solute with encouraging results.

DOI: 10.1103/PhysRevE.64.021512

PACS number(s): 61.20.Gy, 61.25.Em

I. INTRODUCTION

When a hydrophobic solute is in an aqueous solution, the unfavorable interaction between solute and solvent can lead to the solute adjusting its configuration to minimize its solvent exposed area. This is frequently mentioned as the driving force for protein folding [1]. To quantify these notions, several simulation and theoretical studies of the hydrophobic effect have appeared [2–7]. Among them, the theory of Lum, Chandler, and Weeks (LCW) on the hydrophobic effect predicted interesting consequences when the solute is sufficiently large. Specifically, LCW predicted the formation of a vapor layer in the immediate vicinity of the solute. The implications of these results are still being debated.

The ideas of LCW and others can naturally be cast in a simple picture based on the density functional theory (DFT) description of liquids. It is our purpose to construct a DFT that unifies the theories on hydrophobicity. There is a large body of work on DFT of liquids [8,9], mostly for Lennard-Jones (LJ) like fluids. The usual approach is based on the thermodynamic perturbation theory (TPT) [10]. The interaction potential, $\phi(r)$, of the LJ particles can be decomposed into a reference part plus a perturbative part

$$\phi(r) = \phi_0(r) + \phi_a(r). \quad (1.1)$$

The reference system represented by ϕ_0 is usually taken to be a hard-sphere fluid of proper size. Using thermodynamic perturbation theory, the Helmholtz free energy functional can be written as

$$F[\rho(\mathbf{r})] = F_0[\rho(\mathbf{r})] + \frac{1}{2} \int_0^1 d\alpha \int d\mathbf{r} \int d\mathbf{r}' \rho^{(2)}(\mathbf{r}, \mathbf{r}'; \phi_\alpha) \times \phi_a(\mathbf{r} - \mathbf{r}'), \quad (1.2)$$

where F_0 is the density functional of the hard-sphere fluid defined by ϕ_0 and $\rho^{(2)}$ is the two-body correlation function for the reference system with fixed $\rho(\mathbf{r})$ and external potential ϕ_α ,

$$\phi_\alpha = \phi_0 + \alpha \phi_a. \quad (1.3)$$

Mean field approximation for the second part of Eq. (1.2) is

often assumed; taking $\rho^{(2)}(\mathbf{r}, \mathbf{r}')$ to be approximately $\rho(\mathbf{r})\rho(\mathbf{r}')$, one then obtains

$$F[\rho(\mathbf{r})] = F_0[\rho(\mathbf{r})] + \frac{1}{2} \int d\mathbf{r} \int d\mathbf{r}' \rho(\mathbf{r}) \phi_a(\mathbf{r} - \mathbf{r}') \rho(\mathbf{r}'). \quad (1.4)$$

$F_0[\rho(\mathbf{r})]$ is the density functional for the hard-sphere reference fluid. It is still an active area of research where sophisticated derivation of such a density functional from geometric arguments seems to be possible [11]. One of the more practical minded approach on this subject is pioneered by Tarazona [12]. The idea behind this DFT is the construction of a weighted density functional that correctly matches with the known functional derivatives of the free energy with respect to the density in the uniform limit. In particular, the Percus-Yavick approximation [13] for $c(r)$ can be used to explicitly solve for the weighting functions. This idea of matching the density functional with known $c(r)$ is also pointed out by Curtin and Ashcroft [14].

The use of thermodynamic perturbation theory is based on an important aspect of the LJ system. For dense and close to uniform LJ fluid, the density is largely determined by repulsive forces, or F_0 [15]. In this limit, the attractive part of the functional simply contributes as an energy density and does not effect the fluid density. When the fluid becomes nonuniform, the attractive part is responsible for the formation of interfaces and surface tension. For a molecular fluid however, the situation is significantly different. The structure of dense and uniform molecular fluid is not solely determined by the hard-core part of the potential. A well known example of this is liquid water where the the hydrogen bond network has a strong influence on the liquid structure. Others have used the TPT approach to incorporate orientational information in water interfaces [16]. However, these theories are meant for the large length scale limit and cannot describe molecular scale density variations. Our approach in this paper does not utilize quantities from the water-water interaction potential. Rather, we use known thermodynamic information of water to predict spatial densities and interfacial profiles in the presence of a solute. We show that one is able to treat the molecular liquids in a fashion very similar to simple fluids. Specifically, we show that the weighted density

functional approach can be robustly applied using experimentally observed liquid structure. The density functional is required to reproduce molecular length scale fluctuations. In the large length scale limit such as interfaces, it becomes a van der Waals like theory and reproduces the correct surface tension. Therefore, it is a theory for $\rho(\mathbf{r})$ on all length scales.

The theory proposed in this paper has physical ideas originating from the LCW [4] treatment of hydrophobic interaction that followed the works of Chandler and Pratt [17,18,2,3] on the theory of hydrophobicity and of Weeks *et al.* [5] on the concept of an unbalancing potential. These authors examined the behavior of LJ and water in the presence of a hard-sphere solute. The physical picture that emerged from these investigations lead us to the recognition that a density functional theory utilizing only spatial densities of molecular fluids is indeed possible. The theory presented here therefore combines and extends these previous treatments on the hydrophobic effect. Since it also has general application to other liquids given the proper input information, we have called it a theory for the solvophobic phenomena.

II. QUALITATIVE BEHAVIOR OF NONUNIFORM MOLECULAR FLUIDS

The density functional of Eq. (1.4) predicts the behavior of LJ fluids very well over a range of densities. However, instead of the actual interaction potential of LJ particles, ϕ_a should be an effective attractive potential that is in principle temperature and density dependent [19]. Indeed, given a proper choice of ϕ_a , this DFT describes the formation of *interfaces* quite well. This is because it makes a direct connection with the van der Waals' theory of liquid-vapor interface. In the limit of $\rho(\mathbf{r})$ being a smooth function of \mathbf{r} , i.e., it does not change very much over a correlation length in the fluid, Eq. (1.4) can be approximated by

$$F[\rho(\mathbf{r})] = \int d\mathbf{r} \Phi[\rho(\mathbf{r})] + \frac{1}{2} \int d\mathbf{r} \int d\mathbf{r}' \rho(\mathbf{r}) \times \phi_a(\mathbf{r}-\mathbf{r}') \rho(\mathbf{r}'), \quad (2.1)$$

where $\Phi[\rho]$ is the hard-sphere equation of state. Equation (2.1) is exactly the van der Waals' free energy functional. Therefore, Eq. (1.4) is an interpolation between the uniform fluid and the interface limit. Within the van der Waals' theory, the exact form of ϕ_a is also not crucial, rather the energy density parameter a defined as

$$a = -\frac{1}{2} \int d\mathbf{r} \phi_a(r) \quad (2.2)$$

and the range of the attraction m defined as

$$m = -\frac{1}{6} \int d\mathbf{r} r^2 \phi_a(r) \quad (2.3)$$

are more relevant for the surface tension. After making a gradient expansion of $\rho(\mathbf{r}')$ around \mathbf{r} , Eq. (2.1) is essentially equivalent to the functional

$$F[\rho(\mathbf{r})] = \int d\mathbf{r} \Phi[\rho(\mathbf{r})] - a\rho^2(\mathbf{r}) + \frac{1}{2} m |\nabla \rho(\mathbf{r})|^2. \quad (2.4)$$

Here, both a and m are temperature dependent quantities.

For a molecular fluid such as water, the density field in principle is a function of space as well as orientation, i.e., $\rho(\mathbf{r}, \mathbf{\Omega})$. In the case of water, for example, \mathbf{r} labels the position of the oxygen atom and $\mathbf{\Omega}$ describes the orientation of the molecular dipole. For such a system, there is a potential function $V(\mathbf{r}_1, \mathbf{\Omega}_1, \mathbf{r}_2, \mathbf{\Omega}_2, \dots)$ that completely specifies the interaction between molecules. Given this potential energy, the grand potential is defined in the usual way and a molecular free energy density functional exist for $V(\mathbf{r}_1, \mathbf{\Omega}_1, \mathbf{r}_2, \mathbf{\Omega}_2, \dots)$ from standard arguments. However, if we integrate over $\mathbf{\Omega}_i$, a temperature dependent effective potential can be obtained for the spatial degrees of freedom

$$V_{\text{eff}}(\mathbf{r}_1, \mathbf{r}_2, \dots) = \frac{1}{\beta} \ln \left[\int d\mathbf{\Omega}_1 d\mathbf{\Omega}_2 \dots e^{-\beta V(\mathbf{r}_1, \mathbf{\Omega}_1, \mathbf{r}_2, \mathbf{\Omega}_2, \dots)} \right]. \quad (2.5)$$

For V_{eff} , a grand potential can be defined by integrating over the space variables and the resulting density functional depends on the spatial density $\rho(\mathbf{r})$ alone. Having integrated out the orientational degrees of freedom, this functional contains less information and cannot describe any phenomena related to orientational ordering. Nevertheless, it can be made to describe the spatial densities in some detail.

The form of this simplified spatial density functional might be quite generic for all molecular fluids. For uniform densities, there is a functional that describes liquid structure just as F_0 approximately describes the uniform LJ fluid. And in order to describe the formation of interfaces, one must add an energy density term as it is done in Eq. (1.4). Therefore, we write the functional as

$$F[\rho(\mathbf{r})] = F_0[\rho(\mathbf{r})] + \frac{1}{2} \int d\mathbf{r} \int d\mathbf{r}' \rho(\mathbf{r}) \phi_m(\mathbf{r}-\mathbf{r}') \rho(\mathbf{r}'). \quad (2.6)$$

Here, ϕ_m should not be regarded as an actual attractive potential of the molecular fluid, rather it is a quantity that can be adjusted to match the observed thermodynamics properties. In fact, the energy density part should be regarded as equivalent to $-a\rho^2(\mathbf{r}) + \frac{1}{2} m |\nabla \rho(\mathbf{r})|^2$ in Eq. (2.4). Equation (2.6) is again an interpolation from the uniform limit to the interface limit. F_0 must be consistent with the observed $c(r)$ in the uniform limit. This can be accomplished using the weighted density functional procedure explained in the next section. As it is with the LJ fluid, the exact form of ϕ_m should be unimportant and the a and m values of ϕ_m must be consistent with the interface and observed surface tension.

In order to see that Eq. (2.6) has a physical basis, we draw upon some recent observations of nonuniform fluids. Several groups have examined the behavior of water [4,2,6] and LJ [5,7] fluids in the presence of a hard-sphere solute. This situ-

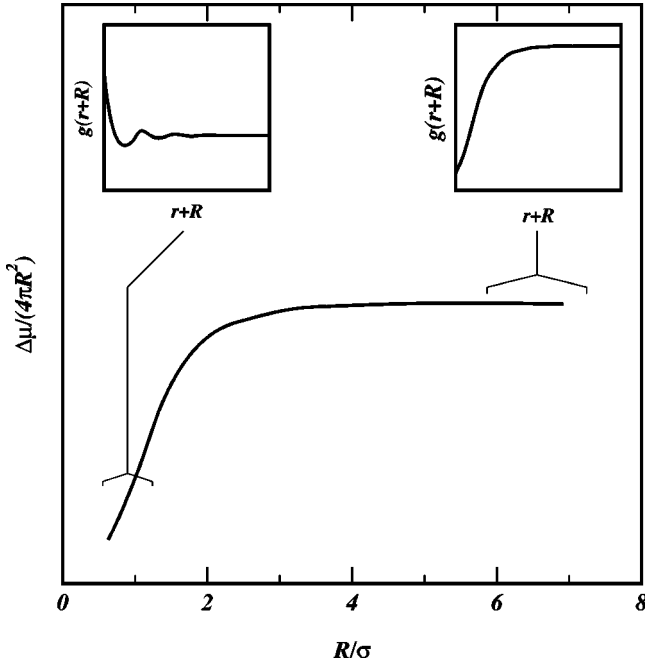


FIG. 1. A schematic depiction of the excess chemical potential (solvation energy) of a hard-sphere solute of radius R in a liquid. σ is the effective length scale. (For water, σ can be taken to be 2.9 Å.) For small solute sizes (indicated by the bracket), the excess chemical potential is roughly a linear function of the volume of the solute. A typical solute-solvent $g(r)$ is shown in the left insert. One sees that the solvent simply packs around the solute in a manner consistent with χ^{-1} of the uniform liquid. For larger solute sizes, the excess chemical potential is a function of the solute surface area. From the $g(r)$ profile in the right insert, one sees that a vapor-liquid interface like density profile is formed at the edge of the solute. In the $R \rightarrow \infty$ limit, $\Delta\mu/4\pi R^2$ is essentially the surface tension of the vapor-liquid interface of the solvent.

ation is also equivalent to the formation of a cavity of size R in the liquid. The findings are schematically summarized in Fig. 1 where the behavior of the excess chemical potential of solvation is plotted vs the cavity size. Also shown are representative spatial density profiles of the liquid for various cavity sizes. Figure 1 shows that water is indeed very similar to the LJ fluids in several respects. For small cavity sizes, the local structure of the liquid is not disturbed very much and liquid simply rearranges around the cavity. The excess free energy and the spatial density can be determined by a quadratic expansion of the free energy around the uniform density [18,2]. More precisely, for small cavities in water, the free energy functional is approximately

$$F[\rho(\mathbf{r})] \approx \frac{1}{2\beta} \int d\mathbf{r} \int d\mathbf{r}' [\rho(\mathbf{r}) - \rho_l] \chi_w^{-1}(\mathbf{r} - \mathbf{r}') [\rho(\mathbf{r}') - \rho_l] \approx F_0[\rho(\mathbf{r})], \quad (2.7)$$

where $\chi_w^{-1} = \delta\beta F / \delta\rho(\mathbf{r})\delta\rho(\mathbf{r}')$ at ρ_l for water [20]. For larger cavities however, the fluid will deviate from the Gaussian behavior implied by Eq. (2.7) [7]. A liquid molecule near the large void will experience a net attraction to the bulk or net repulsion away from the cavity. Density is

depleted from the edge of the cavity and drying occurs. Weeks *et al.* [5] and Lum *et al.* [4] describe this with an unbalancing force. Eventually a liquid-vapor interface is formed. In this limit, LCW showed that a van der Waals like free energy functional describes the smooth density profiles of water quite well:

$$F[\rho(\mathbf{r})] = \int d\mathbf{r} W[\rho(\mathbf{r})] + \frac{1}{2} \int d\mathbf{r} \int d\mathbf{r}' \rho(\mathbf{r}) \times \phi_m(\mathbf{r} - \mathbf{r}') \rho(\mathbf{r}'), \quad (2.8)$$

where $W[\rho]$ is a simple equation of state for a finite sized ideal gas. This is the analog of Eq. (2.1) for the Lennard-Jones case. (For ϕ_m , LCW did not take an explicit functional form, rather they used experimentally determined a and m values from the surface tension.)

The results of these investigations indicate that the generic functional form of Eq. (2.6) should be adequate for the aqueous solvent. Equation (2.6) might even be correct for other molecular fluids where the solvent molecules are “small” and do not exhibit strong spatial orientational effects. The detail inputs that make it quantitative is explained in the next section.

III. CONSTRUCTING A DENSITY FUNCTIONAL THEORY

The spatial density functional of the fluid therefore must match with three observed water properties. The trivial limit is the homogeneous limit where the free energy is given by the equation of state,

$$F[\rho] = \int d\mathbf{r} \{W[\rho] - a\rho^2\}, \quad (3.1)$$

where $W[\rho]$ is the equation of state without the energy density contribution. Thus, in the uniform limit F_0 in Eq. (2.6) should reduce to $\int d\mathbf{r} W(\rho)$ and $\frac{1}{2} \int d\mathbf{r} d\mathbf{r}' \rho(\mathbf{r}) \phi_m(\mathbf{r} - \mathbf{r}') \rho(\mathbf{r}')$ should reduce to $-\int d\mathbf{r} a\rho^2$. $W[\rho]$ must naturally correspond to the observed equation of state for the fluid, although the detailed functional form is quite arbitrary. The other two limits are the interface limit where the free energy is given by Eq. (2.8) and the small deviation limit where the free energy is quadratic. To interpolate between Eqs. (2.7) and (2.8), we use a weighted density functional of the form,

$$F_0[\rho(\mathbf{r})] = F_{id}[\rho(\mathbf{r})] + \int d\mathbf{r} \rho(\mathbf{r}) \Psi[\bar{\rho}(\mathbf{r})], \quad (3.2)$$

where F_{id} is the free energy density of an ideal gas

$$F_{id}[\rho(\mathbf{r})] = \int d\mathbf{r} \rho(\mathbf{r}) k_B T [\ln \rho(\mathbf{r}) - 1], \quad (3.3)$$

and $\bar{\rho}$ is the weighted density determined by the self consistent equation

$$\bar{\rho}(\mathbf{r}) = \int d\mathbf{r}' \rho(\mathbf{r}') w[\mathbf{r} - \mathbf{r}'; \bar{\rho}(\mathbf{r})], \quad (3.4)$$

where $w[\mathbf{r}-\mathbf{r}';\bar{\rho}(\mathbf{r})]$ is the weighting function. $\Psi[\rho]$ in this case must satisfy

$$W[\rho]=\rho k_B T(\ln \rho-1)+\rho\Psi[\rho]. \quad (3.5)$$

For water, we have taken $W[\rho]$ to be

$$W[\rho]=\rho k_B T \log\left[\frac{b\rho}{1-b\rho}\right], \quad (3.6)$$

where $a=229$ kJ cm³/mol, $b=14.99$ cm³/mol at 298 K [4]. This parametrization is based on a fit to water compressibility and the density difference between liquid and gas. At best it is a very crude approximation to the actual water properties. Other forms of $W[\rho]$ that can give a better fit of water phase boundary and equation of state will undoubtedly yield better results.

With the proper choice of the weighting function, one sees that if $\rho(\mathbf{r})$ is a smooth function of space, then $\bar{\rho}(\mathbf{r})\approx\rho(\mathbf{r})$, we obtain the van der Waals limit of Eq. (2.8). Now we determine the weighting function using Eq. (2.7).

A. The weighting functions

The strategy we employ for determining F_0 and the weighting functions is to match known $c(r)$'s with the second derivatives of the free energy in Eq. (3.2). Since

$$c(|\mathbf{r}-\mathbf{r}'|)=\left.\frac{\delta\beta(F_0-F_{id})}{\delta\rho(\mathbf{r})\delta\rho(\mathbf{r}')}\right|_{\rho_l}, \quad (3.7)$$

[here, we have made the definition that $c(r)$ contains no attractive interaction] taking the second derivative with respect to $\rho(\mathbf{r})$ of Eq. (3.2) and setting the density to the uniform density gives the following expression for $c(r)$:

$$\begin{aligned} c(|\mathbf{r}-\mathbf{r}'|) &= -\frac{2\Psi'(\rho_l)}{k_B T} w(|\mathbf{r}-\mathbf{r}'|;\rho_l) \\ &\quad -\frac{\rho_l\Psi''(\rho_l)}{k_B T} \int d\mathbf{r}'' w(|\mathbf{r}''-\mathbf{r}|;\rho_l) w(|\mathbf{r}''-\mathbf{r}'|;\rho_l) \\ &\quad -\frac{\rho_l\Psi'(\rho_l)}{k_B T} \int d\mathbf{r}'' [w'(|\mathbf{r}''-\mathbf{r}|;\rho_l) \\ &\quad \times w(|\mathbf{r}''-\mathbf{r}'|;\rho_l) + w'(|\mathbf{r}''-\mathbf{r}'|;\rho_l) \\ &\quad \times w(|\mathbf{r}''-\mathbf{r}|;\rho_l)]. \end{aligned} \quad (3.8)$$

Written in k space, this equation reads as

$$c(k)=-\frac{2\Psi'(\rho_l)}{k_B T} w(k,\rho_l)-\frac{\rho_l}{k_B T} \frac{\partial}{\partial\rho_l} [\Psi'(\rho_l)w^2(k,\rho_l)]. \quad (3.9)$$

Clearly, because the weighting function depends on ρ_l , one in principle must know the full dependence of $c(k)$ on ρ_l to solve this equation. Usually, this dependence is not known.

In order to make progress, we follow Tarazona's further approximation on the weighting function and express $w(r;\rho)$ as

$$w(r,\rho)=w_0(r)+w_1(r)\rho+w_2(r)\rho^2, \quad (3.10)$$

where $w_i(r)$ are *independent* of ρ and temperature. The weighting function must be normalized, i.e.,

$$\int d\mathbf{r} w(r)=1. \quad (3.11)$$

We have chosen $w_0(r)$ to be a step function of the form

$$w_0(r)=\frac{3}{4\pi\sigma^3}\Theta(\sigma-r), \quad (3.12)$$

where $\sigma=b^{1/3}=2.89$ Å is the length scale given by the equation of state. Θ is the usual step function. With this choice of $w_0(r)$, $w_1(r)$ and $w_2(r)$ must integrate to zero,

$$\int d\mathbf{r} w_{1,2}(r)=0. \quad (3.13)$$

The simplification that results from the expansion of Eq. (3.10) is twofold. First, the self-consistent equation of Eq. (3.4) can now be solved analytically. The result is [12]

$$\bar{\rho}(\mathbf{r})=\frac{2\bar{\rho}_0(\mathbf{r})}{1-\bar{\rho}_1(\mathbf{r})+[\{1-\bar{\rho}_1(\mathbf{r})\}^2-4\bar{\rho}_0(\mathbf{r})\bar{\rho}_2(\mathbf{r})]^{1/2}}, \quad (3.14)$$

where

$$\bar{\rho}_i(\mathbf{r})=\int d\mathbf{r}' w_i(\mathbf{r}-\mathbf{r}')\rho(\mathbf{r}'). \quad (3.15)$$

Second, the weight functions w_1 and w_2 can be solved from a given set of $c(r)$'s. More precisely, using Eq. (3.9), if one has $c(k)$ at two different condition (ρ_l and temperature), we can introduce coupled equations for these two conditions

$$\begin{aligned} c_1(k) &= -\frac{2\Psi'(\rho_1)}{k_B T_1} w(k,\rho_1) \\ &\quad -\frac{\rho_1}{k_B T_1} \frac{\partial}{\partial\rho_1} [\Psi'(\rho_1)w^2(k,\rho_1)], \\ c_2(k) &= -\frac{2\Psi'(\rho_2)}{k_B T_2} w(k,\rho_2) \\ &\quad -\frac{\rho_2}{k_B T_2} \frac{\partial}{\partial\rho_2} [\Psi'(\rho_2)w^2(k,\rho_2)]. \end{aligned} \quad (3.16)$$

With the two unknowns $w_1(k)$ and $w_2(k)$, two coupled equations are in principle sufficient. If one wants to introduce a cubic order in the expansion in Eq. (3.10), three coupled equations are needed.

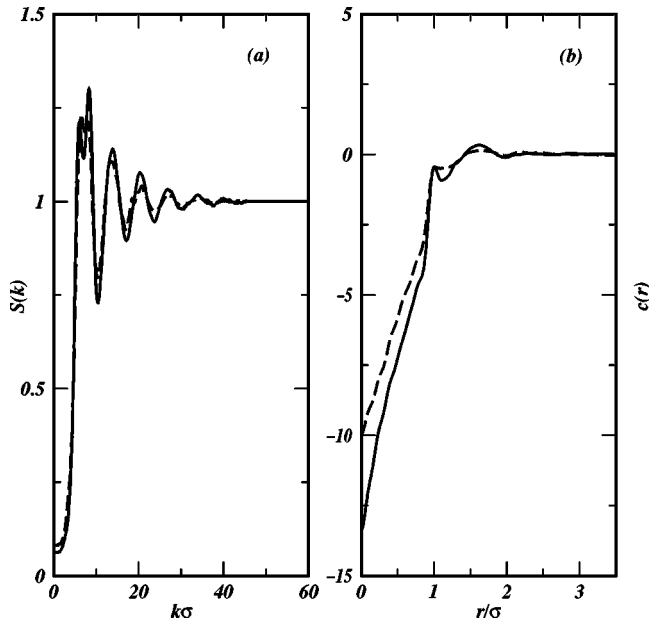


FIG. 2. The experimentally measured (a) $S_{00}(k)$ and (b) $c(r)$ for liquid water at 298 K (solid line) and 373 K (dashed line).

Thus, even though one does not have the $c(k)$ for all densities, using experimental (or simulation) results for $c(k)$ at two different conditions should allow one to search for the weighting functions. The complication is that the coupled equations are *nonlinear*. Therefore, the solutions at a particular k value may not be unique. For certain k 's, solutions may not even exist. Nevertheless, we have carried out a numerical search [21] for the solutions of Eq. (3.16) using experimentally measured $S_{00}(k)$ [22] values for water. The two conditions we have chosen are at 298 K and 373 K. The water densities at these temperatures are 0.997 and 0.958 g/cm³, respectively [23]. The experimentally observed $S(k)$ in principle contains attractive interactions. We have assumed their contributions are small. Figure 2 displays the $S(k)$'s and the $c(r)$'s for these two conditions. The weighting functions obtained from numerical solutions to Eq. (3.16) are displayed in Fig. 3. Roots of the coupled equations are successfully obtained for most k 's. Not shown are the $c(r)$'s calculated from the weighting functions, they are essentially indistinguishable from those in Fig. 2.

As a test of the quality of the weighting functions, we have used them to predict the $c(k)$'s for other density and temperatures. For example, in Fig. 4, we show the experimentally measured $c(k)$'s at 323 K and 423 K vs $c(k)$'s obtained using the weighting function. For these two conditions, the densities are 0.988 and 0.917 g/cm³, respectively. One sees that the comparison is indeed favorable.

B. The energy density part

As we explained in Sec. II, $\phi_m(r)$ must satisfy several constraints. First, in order to match the equation of state, the potential must satisfy

$$-\frac{1}{2} \int d\mathbf{r} \phi_m(r) = a. \quad (3.17)$$

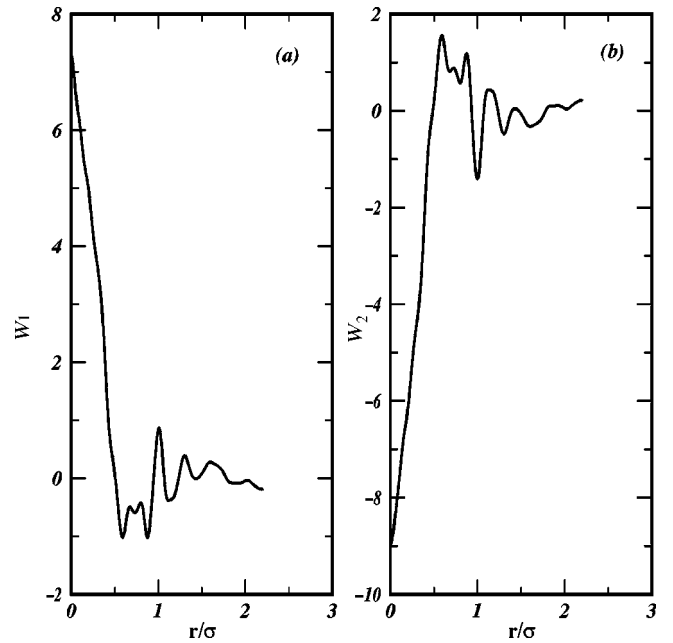


FIG. 3. The weighting functions obtained from solutions of Eq. (3.16). (a) $w_1(r)$ and (b) $w_2(r)$.

Second, the surface tension γ obtained from the DFT must also match with the experimental value of 0.072 J/m². Within the van der Waals' theory of surface tension, γ is proportional to the square root of m [Eq. (2.3)], which is essentially a measure of the range of the attractive potential. Therefore one can simply adjust the value of m to produce the desired γ .

These two constraints are clearly not enough to determine the functional form of the potential. However, the detailed

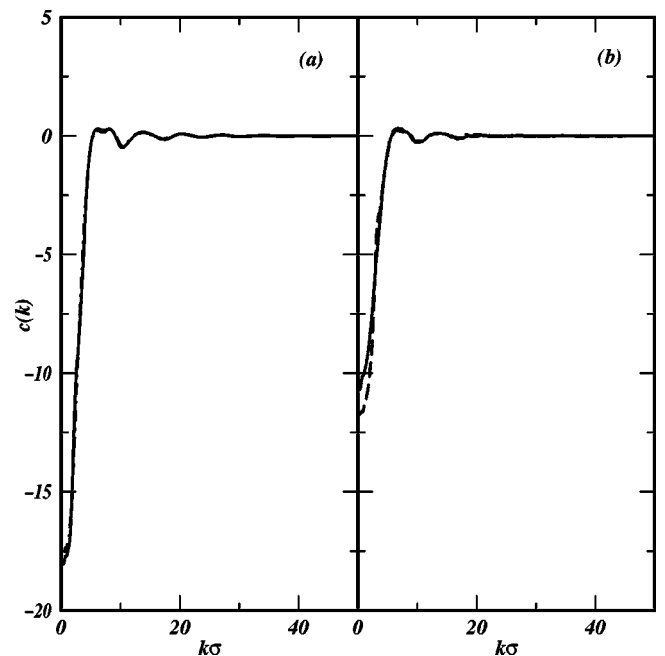


FIG. 4. Experimentally measured $c(k)$'s (dotted lines) compared with those calculated (solid lines) using the weighting functions (a) 323 K and (b) 423 K.

functional form is not crucial. One could simply take the energy density part of the functional in Eq. (2.6) as

$$\int d\mathbf{r} -a\rho(\mathbf{r})^2 + \frac{1}{2}m|\nabla\rho(\mathbf{r})|^2. \quad (3.18)$$

Another alternative is to choose a potential that matches with the desired a and m values. For example, we have performed calculations below using a ϕ_m of the form

$$\phi_m(r) = \begin{cases} -\epsilon, & r < \sigma \\ \epsilon\left(\frac{r-\sigma}{d-\sigma} - 1\right), & \sigma < r < d \\ 0, & r > d, \end{cases} \quad (3.19)$$

where ϵ and d can be solved by knowing a and m . Calculations in next section show that taking other forms of the potential does not make any significant difference in the final results.

We note that since ϕ_m is made to match a and m at 298 K, it should be different for other temperatures. Therefore, out density functional cannot predict the temperature dependence of γ . If the temperature dependence of m and a are known, then one can adjust ϕ_m accordingly. This problem is also present in the LJ functional of Eq. (1.4) where ϕ_a in principle does not have any temperature information.

IV. TEST CALCULATIONS

A. Cavity formation in liquid water

Equations (2.6), (3.2), and (3.19) completely specify our density functional. To test its accuracy, we have carried out a calculation for liquid water with the presence of a spherical void. This example nicely demonstrates water density variations on all length scales. Our results will be compared with some computer simulation results [2,6] below. Due to spherical symmetry, ρ is a function of the one dimensional variable r . The weighted density is calculated from Eq. (3.4) and it is zero inside the cavity. The equilibrium density is the solution to the equation

$$\frac{\delta F[\rho(r)]}{\delta \rho(r)} = \mu, \quad (4.1)$$

where the chemical potential is

$$\mu = \left. \frac{\delta F[\rho(r)]}{\delta \rho(r)} \right|_{\rho(r)=\rho_l}. \quad (4.2)$$

In practice, follow the direction of the functional derivative until it equals μ . The excess chemical potential of creating a cavity of size R in liquid water defined as

$$\Delta\mu(R) = F(R) - F(0), \quad (4.3)$$

where $F(0)$ is the free energy of the uniform liquid without a cavity and $\Delta\mu(R)$ is also the excess chemical potential of solvating a hard sphere of radius R in water.

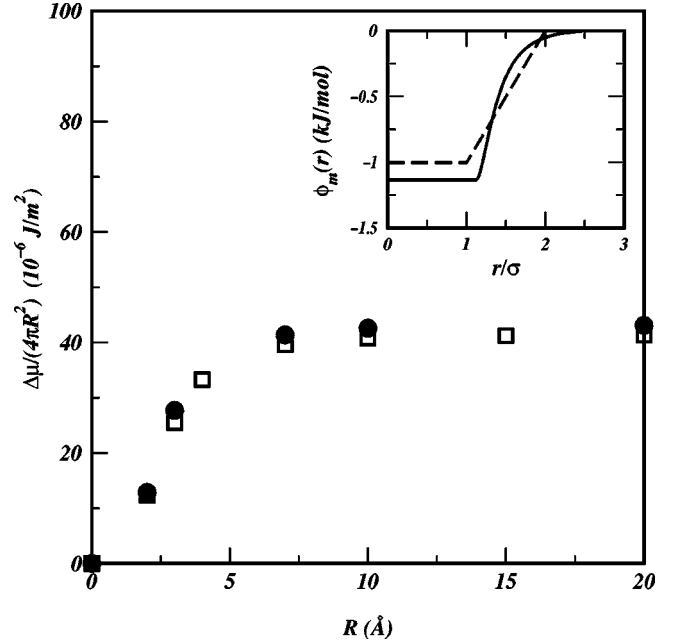


FIG. 5. The excess chemical potential of a cavity in water calculated using density functional theory with two different attractive potentials (shown in the insert). These potentials have the same a and m values and give essentially the same excess chemical potential. Here, R refers to the size of the cavity.

First, to show that the functional form of ϕ_m is not important for the DFT, we have performed calculations of $\Delta\mu(R)$ for two different potentials. One is in the form of Eq. (3.19) and the other is in the form of a truncated LJ potential. These two potentials not only have exactly the same a value, they also possess very similar values of m . In Fig. 5, $\Delta\mu(R)$ and the asymptotic surface tension for these two potentials are essentially identical. The densities obtained for all cavity sizes are also indistinguishable for these potentials. Therefore, any reasonable ϕ_m with the proper a and m values are probably adequate.

The value of d in Eq. (3.19) that agrees well with the experimentally observed surface tension at 298 K is $d = 3.0\sigma$ or 8.6 Å, giving $m = 2.3 \times 10^{-10} \text{ J/mol}^2 \text{ cm}^5$. The comparison of $\Delta\mu(R)$, experimentally observed surface tension is shown in Fig. 6. The DFT surface tension with these parameters is 0.070 J/m². LCW used a m value of $3.3 \times 10^{-10} \text{ J/mol}^2 \text{ cm}^5$, giving a surface tension of about 0.082 J/m². The ratio of the square roots of these m values is in accordance with the the ratio of the surface tensions obtained, confirming that both LCW and DFT are reproducing van der Waals' theory at the interface limit.

Finally, the water density around a cavity size of 3 Å compared to a SPC water simulation is shown in Fig. 7. One clearly sees that the packing behavior of water at the boundary of the cavity is roughly correct. We also show the water densities for larger cavity sizes in Fig. 8, demonstrating the formation of an interface at the edge of the cavity. There is simulation data available for the cavity-solvent $g(r)$ contact values [2,6]. The comparison is shown in Fig. 9. One sees that the DFT result is roughly in agreement with simulations,

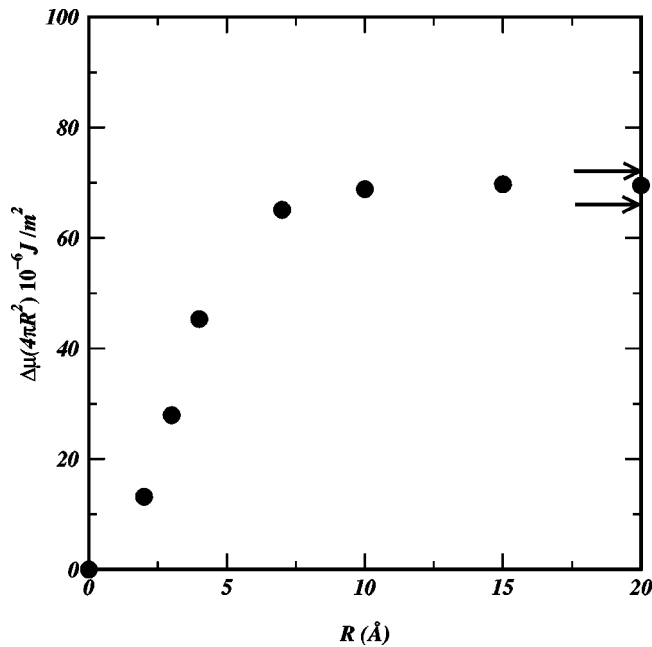


FIG. 6. The excess chemical potential of a cavity in water as function of the cavity radius R . d parameter in Eq. (3.19) is taken to be 3.0σ that gives the desired m value. The arrows at 0.072 J/m^2 are the liquid-vapor surface tension from experiments. The arrow at 0.066 J/m^2 is the surface tension of SPC/E water from simulations [24]. R is the radius of the cavity.

given the crudeness of the equation of state in Eqs. (3.1) and (3.6).

The DFT results are in qualitative agreement with the predictions of LCW theory. One clearly sees the formation of a liquid-vapor interfaces as the solute become large. (In the

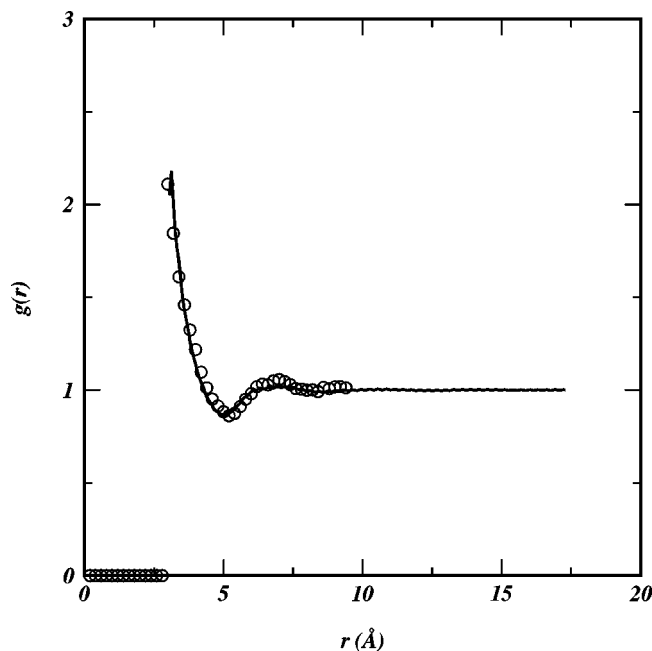


FIG. 7. The cavity-solvent $g(r)$ obtained from the density functional calculation. The cavity size R is 3 \AA . The simulation results (circles) are obtained using the SPC parametrization of water.

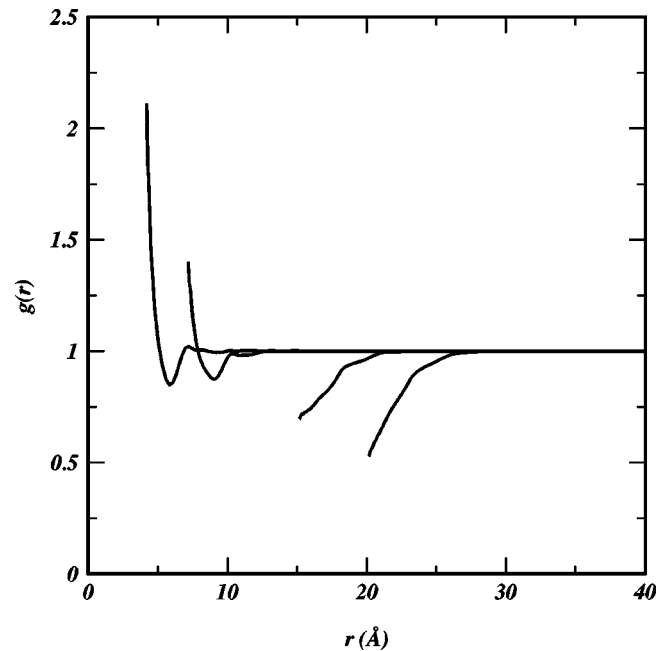


FIG. 8. The cavity-solvent $g(r)$ obtained from the density functional calculations. The cavity sizes range from 4 to 20 \AA .

next section, we show a density profile near an infinite planar solute.) The advantages of DFT are that the densities and free energies are all obtained from the same functional. The calculations are generally much simpler than what are required for LCW.

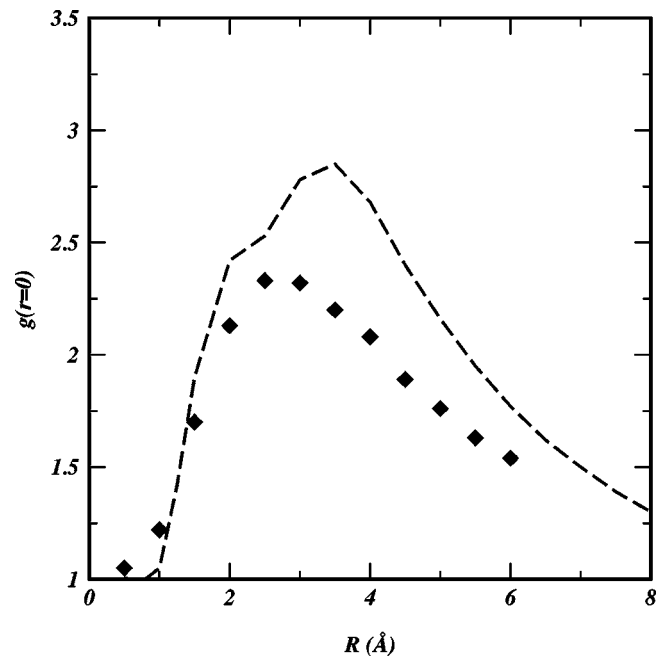


FIG. 9. The cavity-solvent $g(r)$ contact values from the DFT calculation (dashed line) vs simulations/fitting result of Hummer *et al.* [2] and Floris *et al.* [6]. This graph is an analog of Fig. 2(b) in Ref. [15].

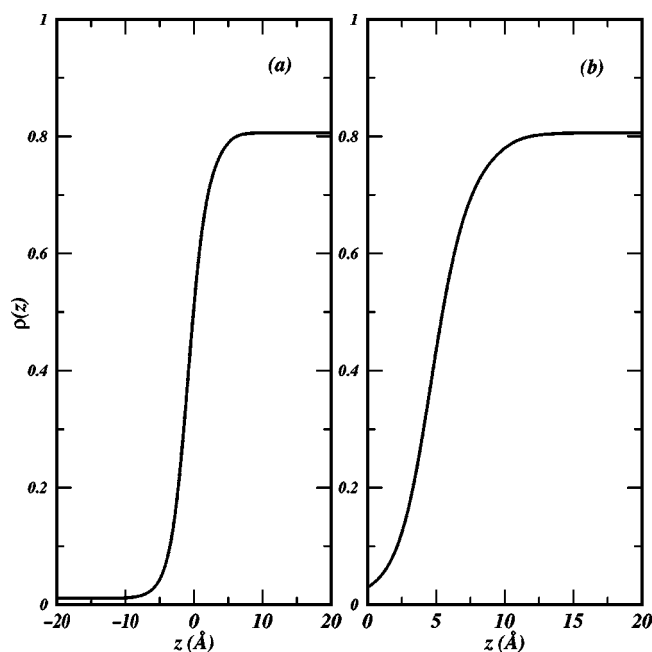


FIG. 10. (a) Density functional results of a free liquid-vapor interface at 298 K. It is obtained by fixing the asymptotic density to liquid and vapor values. (b) The liquid densities at a hard wall are in units of σ^3 . One sees that a vaporlike layer exists between the bulk and the wall.

B. Interfacial profiles

We have emphasized that in the large length scale limit, our DFT reduces to the van der Waals' theory of liquids. In Fig. 10, we show an interface obtained from our DFT by fixing the density at $z = \pm\infty$ to be liquid and vapor, respectively. The interface width from our calculation is about 15 \AA . Compared to the simulation results of Alejandro *et al.* [24] the interface is clearly too wide. This is due to the equation of state. Unlike the hard-sphere functional where the Carnahan-Starling equation of state is essentially exact, our equation of state for water is very crude. A better parametrization of $W[\rho]$ is desirable. We are not aware of a comprehensive fit of water equation of state in the literature. A detailed study is probably worthwhile. We note that previous density functional theories of water interface [16] using a mean field like attractive potential also overestimate the interfacial width to some extent.

Also shown in Fig. 10 is the density profile of water at the edge of an infinite solute, i.e., a wall. Our results show that an interfacial profile occurs. This is again in agreement with the LCW theory.

V. DISCUSSION AND CONCLUSIONS

We have presented a theory of solvophobicity based on the weighted density functional approach. The theory has limits that agree with the quadratic free energy functional of Eq. (2.7) as well as the van der Waals' theory of liquid-vapor interface. The DFT can predict spacial density profiles of liquids as well as free energies of solvation. Our results for an ideal hydrophobic solute (i.e., a cavity) show that as the solute becomes larger, a liquid-vapor interface is formed. These results are in qualitative agreement with the findings of LCW. It is also possible to compute the free energy cost of solvating cavities. Our results show that in the infinitely large solute limit, the free energy cost is proportional to the area of the solute. The proportionality constant is the liquid-vapor surface tension. There are also advantages of this theory compared to LCW. For example, unlike the two step process of LCW theory, free energies and density profiles are given by the same free energy expression. Many practical aspects of the calculation are simplified as a result.

For actual hydrophobic solutes such as hydrocarbons, the situation is quite different. There is still a small attraction between the solute and solvent. In this case, the necessary modifications of our DFT consist of an extra term, i.e., one should add to Eq. (2.6) $\int d\mathbf{r}u(\mathbf{r})\rho(\mathbf{r})$, where $u(\mathbf{r})$ is the effective potential between solute and solvent. The density profiles could change substantially as a result. This case will be discussed in more detail elsewhere.

We have also shown how to apply the weighted density functional approach to fluids other than LJ. The DFT does not have to rely on intermolecular potentials. Rather it can be based on experimental observed liquid structure and thermodynamic observables. This gives a well defined recipe to construct the necessary weighting functions. Using Tarazona's polynomial expansion, we solved a coupled equation for which the weight functions are solutions. The DFT is able to predict solvent densities to all length scales. Although the interfacial profiles obtained are somewhat too wide compared to simulations. We attributed this to the crude nature of the equation state used in the DFT. Given an equation of state that can adequately predict interfacial properties of water, the DFT should be much improved.

ACKNOWLEDGMENTS

The author would like to thank Professor David Chandler and Dr. Pieter Rein ten Wolde for many stimulating discussions. The computer simulation results provided by David Huang and Phill Geissler are gratefully acknowledged. This work has been supported by the Director, Office of Energy Research, Office of Basic Energy Sciences, Chemical Sciences Division of the U.S. Department of Energy under Contract No. DE-FG03-87ER13793.

- [1] W. Kauzmann, *Adv. Protein Chem.* **14**, 1 (1959); C. Tanford, *The Hydrophobic Effect-Formation of Micelles and Biological Membranes* (Wiley-Interscience, New York, 1973).
 [2] G. Hummer, S. Garde, A. E. Garcia, A. Pohorille, and L. R.

- Pratt, *Proc. Natl. Acad. Sci. U.S.A.* **93**, 8951 (1996).
 [3] G. Hummer, S. Garde, A. E. Garcia, M. E. Paulaitis, and L. R. Pratt, *J. Phys. Chem. B* **102**, 10469 (1998); G. Hummer, S. Garde, A. E. Garcia, and L. R. Pratt, *Chem. Phys.* **258**, 349

- (2000).
- [4] K. Lum, D. Chandler, and J. D. Weeks, *J. Phys. Chem.* **103**, 4570 (1999).
- [5] J. D. Weeks, K. Katsov, and K. Vollmayr, *Phys. Rev. Lett.* **81**, 4400 (1998).
- [6] F. M. Floris, M. Selmi, A. Tani, and J. Tomasi, *J. Chem. Phys.* **107**, 6353 (1997).
- [7] D. M. Huang and D. Chandler, *Phys. Rev. E* **61**, 1501 (2000).
- [8] R. Evans, in *Fundamentals of Inhomogeneous Fluids*, edited by D. Henderson (Marcel Dekkar, New York, 1992).
- [9] Y. Singh, *Phys. Rep.* **207**, 351 (1991).
- [10] J. S. Rowlinson and B. Widom, *Molecular Theory of Capillarity* (Oxford University Press, New York, 1982).
- [11] Y. Rosenfeld, M. Schmidt, H. Lowen, and P. Tarazona, *Phys. Rev. E* **55**, 4245 (1997).
- [12] P. Tarazona, *Phys. Rev. A* **31**, 2672 (1985).
- [13] J. P. Hansen and I. R. McDonald, *Theory of Simple Liquids* (Academic Press, London, 1986).
- [14] W. A. Curtin and N. W. Ashcroft, *Phys. Rev. A* **32**, 2909 (1985).
- [15] J. D. Weeks, D. Chandler, and H. C. Anderson, *J. Chem. Phys.* **54**, 5237 (1971).
- [16] B. Yang, D. E. Sullivan, B. Tjijte-Margo, and C. G. Gray, *Mol. Phys.* **76**, 709 (1992); B. Yang, D. E. Sullivan, and C. G. Gray, *J. Phys.: Condens. Matter* **6**, 4823 (1994).
- [17] D. Chandler and L. R. Pratt, *J. Chem. Phys.* **65**, 2925 (1976); L. R. Pratt and D. Chandler, *ibid.* **66**, 147 (1977).
- [18] D. Chandler, *Phys. Rev. E* **48**, 2898 (1993).
- [19] S. Toxvaerd, *J. Chem. Phys.* **55**, 3116 (1971).
- [20] Under certain conditions, the functional of Eq. (2.7) permits unphysical results such as negative densities. Including higher orders expansions in the DFT is difficult and does not yield better results. However, when applied to densities close to ρ_l , including cases of small solutes, the Gaussian functional does correctly predict liquid structure. Theory of Hummer *et al.* [2,3], though has many features similar to Eq. (2.7), does not have this deficiency. See M. A. Gomez, L. R. Pratt, G. Hummer, and S. Garde, *J. Phys. Chem.* **103**, 3520 (1999); L. R. Pratt, G. Hummer, and S. Garde in *New Approaches to Problems in Liquid State Theory*, edited by C. Caccamo, J.-P. Hansen, and G. Stell (Kluwer, Netherlands, 1999).
- [21] W. H. Press, S. A. Teukolsky, W. I. Vetterling and B. P. Flannery, *Numerical Recipes* (Cambridge University Press, Cambridge, England, 1992). The solutions to the coupled equations are searched with the Newton-Raphson method described in Sec. 9.6.
- [22] A. H. Narten and H. A. Levy, *J. Chem. Phys.* **55**, 2263 (1971); The relationship between $c(k)$ and $S(k)$ is $c(k) = 1/\rho_l - 1/\rho_l S(k)$. See Ref. [13].
- [23] *CRC Handbook of Chemistry and Physics*, 67th ed., edited by R. C. Weast (CRC, Boca Raton, FL, 1986).
- [24] J. Alexandre, D. Tildesley, and G. A. Chapela, *J. Chem. Phys.* **102**, 4574 (1995).